Algorithms for sensor-based redistribution of nitrogen fertilizer in winter wheat

J. Berntsen · A. Thomsen · K. Schelde · O. M. Hansen · L. Knudsen · N. Broge · H. Hougaard · R. Hørfarter

Abstract   Several methods were developed for the redistribution of nitrogen (N) fertilizer within fields with winter wheat (*Triticum aestivum* L.) based on plant and soil sensors, and topographical information. The methods were based on data from nine field experiments in nine different fields for a 3-year period. Each field was divided into 80 or more subplots fertilized with 60, 120, 180 or 240 kg N ha^{-1}. The relationships between plot yield, N application rate, sensor measurements and the interaction between N application and sensor measurements were investigated. Based on the established relations, several sensor-based methods for within-field redistribution of N were developed. It was shown that plant sensors predicted yield at harvest better than soil sensors and topographical indices. The methods based on plant sensors showed that N fertilizer should be moved from areas with low and high sensor measurements to areas with medium values.The theoretical increase in yield and N uptake, and the reduced variation in grain protein content resulting from the application of the above methods were estimated. However, the estimated increases in crop yield, N-uptake and reduced variation in grain protein content were small.

Keywords   EM38 · Nitrogen redistribution · Spectral measurements · Topography · Yara N-sensor

Introduction

The within-field variation in yield observed with yield-mapping technology is often large (e.g. Joernsgaard & Halmoe, 2003). Precision farming aims to use this observed variation to increase yield and N uptake, reduce variation in protein content, and so on, by varying

J. Berntsen · A. Thomsen (✉) · K. Schelde · N. Broge · H. Hougaard
Department of Agroecology, Danish Institute of Agricultural Sciences, P.O. Box 50, DK-8830 Tjele, Denmark
e-mail: Anton.Thomsen@agrsci.dk

O. M. Hansen · L. Knudsen · R. Hørfarter
National Centre, Crop Production, Danish Agricultural Advisory Service, Udkærsvej 15, DK-8200 Århus N, Denmark

the application rate of fertilizers and pesticides. Variable rate application of N fertilizer is especially interesting in a precision farming framework because of the potential economic and environmental benefits.

During the last decade, several soil (Heiniger, McBride, & Clay, 2003) and plant (Wollring, Reusch, & Karlsson, 1998) sensors have become available for mapping field variability. By combining sensor measurements, historical yield maps, topographic information, variable rate technology (VRT), and global positioning systems (GPS), it is possible to implement variable fertilizer applications on fields of even moderate size (e.g. Lund, Wolcott, & Hansen, 2001). The fundamental question is how to optimize the distribution of N fertilizer within a field based on sensor measurements and other available sources of information. A few methods exist to do this (e.g. Flowers, Weisz, & Heiniger, 2003; Lukina et al., 2001; Lund et al., 2001), but often they have not been tested under a sufficient range of conditions.

In general, variable rate methods of N application can be divided into two groups: redistribution of a predefined total amount of N or determination of the site-specific N demand. The former requires knowledge of the field variation, whereas this is unnecessary for the demand methods. The latter is more difficult to develop, however, as it requires inter-field and inter-annual variation to be described. In practice, this is sometimes accomplished by treating small plots differently from the rest of the field. For example, Raun et al. (2002) fertilized a strip within a field at a rate of N that was non-limiting. The normalized difference vegetation index (NDVI) values from this strip were used to make a relative map of NDVI for the whole field.

The aim of the current study was to develop methods for the redistribution of N fertilizer based on information from plant and soil sensors, together with topographic information. In addition, the resulting theoretical yield increase obtained using these methods will be estimated.

Materials and methods

Field sites

During 2001, 2002, and 2003, trials were conducted in nine fields on commercial farms with winter wheat (Table 1). The sites were selected because of their large variability in soil texture and yield potential. Soil apparent electrical conductivity (EC_a) measurements

Table 1 Location, geographical coordinates, number of rows and columns and average soil classification, for the trial sites

Field	Location	Position	Rows	Columns	Plots	Length of plot (m)	Soil classification
1	Vindum	62°48′ N, 53°62′ E	20	6	120	300	Loamy sand
2	Bidstrup	62°44′ N, 55°79′ E	40	6	240	600	Loamy sand
3	Kasted	62°32′ N, 57°03′ E	20	4	80	300	Loamy sand
4	Langaa	62°48′ N, 55°39′ E	24	6	144	360	Sandy loam
5	Hadsten	62°42′ N, 56°23′ E	21	6	126	315	Loamy sand
6	Egeskov	61°15′ N, 59°63′ E	23	6	138	345	Loamy sand
7	Vinkel	62°53′ N, 53°22′ E	20	5	100	300	Loamy sand
8	Trige	62°39′ N, 57°17′ E	20	6	120	300	Loamy sand
9	Funder	62°22′ N, 52°81′ E	20	6	120	300	Loamy sand

were used as an indicator of soil textural variation. The average soil type in the selected fields was loamy sand or sandy loam. The variation in EC_a within the trial areas is given in Table 2, together with plot height, slope and aspect.

The trials were carried out in fields subject to standard farm management practices. All trial areas had typical Danish cereal crop rotations with winter oil seed rape or peas every 5–6 years. Pig or cattle slurry had been applied in previous years to most of the trial areas.

Plot experiments

The general experimental layout is shown in Fig. 1. For each row 60, 120, 180 and 240 kg N ha^{-1} were applied in a randomized way. In some of the trials 180 kg N ha^{-1} were applied to three plots per row to study the variability across the rows. Each plot measured 12 m×2.5 m. Plots were separated by a 3−m protective zone. The total length of each trial area varied between 300 and 600 m, and there were 80–240 plots in each trial. The design of the experiment enabled the effect of N fertilizer on yield and yield quality to be estimated at different locations within the field.

Nitrogen fertilizer was applied on two dates with a pneumatic full-width spreader. Sixty kg N ha^{-1} were applied to all plots at the beginning of the growing season (between March 15th and April 15th). The second application was timed at Zadoks growth stage 32 (mid May), corresponding to typical Danish fertilizer strategy.

The trial sites had about 20 kg phosphorous, 65 kg potassium and 15 kg sulphate fertilizer applied according to standard fertilizer practice of winter wheat cultivation in Denmark. The trial plots received the same weed and pest control treatments as the surrounding field. They were harvested with a plot harvester. Wheat grains were analyzed for water, starch and protein content with a near infrared transmittance (NIT) instrument (Infratech 1241, Foss Electric, Denmark).

Sensor measurements

The ratio vegetation index (RVI), equivalent to the simple ratio (SR), was measured with a handheld instrument with two dual band radiometers (Skye SKR 1800; Skye Instruments Ltd., UK). The narrow (10 nm) spectral bands were centered at 650 nm (red) and 800 nm (near infrared). The RVI index was calculated as the ratio between near-infrared reflectance and red reflectance. The RVI measurements were made on three to four dates during the growing season, starting in early May. The data analysis includes only the measurements made in early May, just prior to the second N-application at growth stage 32–34 (Zadoks, Chang, & Konzak, 1974).

Soil EC_a was measured to a depth of approximately 150 cm (vertical mode) with a Geonics EM38DD sensor (Baden, Williams, & Hoey, 1987, Greve, 2003) mounted on a sledge and towed behind a light vehicle. The sledge was equipped with a Real Time Kinematic Global Positioning System (RTK-GPS; Trimble 5700; Trimble, US).

The Yara N-sensor is a commercially available sensor system (Yara International ASA, Norway) that measures canopy light reflection and estimates an optimum N application rate. Information on the waveband intervals of the reflection measurements was not available, but it was assumed that the estimated biomass was comparable to estimates based on RVI measurements. The tractor-mounted Yara N-sensor measured canopy reflection on both sides of the vehicle. The N-sensor biomass measurements were made in early May, just before the second N-application.

Table 2 Mean, 5% and 95% percentiles of wheat yield, protein content, N uptake, topographic indices and different sensor measurements for each field

	1	2	3	4	5	6	7	8	9
Yield (Mg ha^{-1})	9.5 (7.6–10.6)	8.7 (6.9–10.0)	8.2 (5.8–10.2)	4.7 (3.6–5.6)	6.5 (4.5–8.3)	5.6 (2.8–8.3)	7.4 (5.7–8.4)	7.2 (6.0–8.3)	5.8 (3.4–7.9)
Protein (%)	10.8 (8.7–12.5)	11.1 (8.6–13.0)	10.8 (7.8–13.6)	13.6 (10.6–15.5)	11.8 (8.2–14.3)	10.7 (7.6–12.9)	11.5 (9.3–13.1)	12.1 (8.8–14.5)	13.8 (11.3–15.9)
N uptake (kg N ha^{-1})	167 (107–209)	154 (97–196)	145 (76–213)	104 (62–135)	125 (64–172)	96 (38–160)	137 (90–168)	140 (93–175)	126 (75–175)
Plot height (m)	100 (98–102)	93 (89.7–96.5)	45 (40–49)	24 (14–28)	60 (58–62)	66 (64–67)	77 (73–81)	98 (97–99)	138 (136–141)
Slope (%)	3.1 (0.8–6.5)	3.3 (0.8–8.4)	–	6.1 (2.7–13.3)	1.6 (0.6–3.3)	1.6 (0.5–2.5)	7.1 (2.4–12.3)	3.4 (1.3–8.1)	4.5 (1.1–10.1)
Aspect (°)	140 (41–270)	191 (78–273)	–	69 (12–162)	265 (40–347)	196 (53–307)	210 (60–343)	216 (28–343)	208 (131–313)
SII[a]	1.02 (0.90–1.12)	1.03 (0.98–1.09)	–	0.92 (0.65–1.13)	0.98 (0.95–1.02)	1.0 (0.98–1.01)	1.02 (0.80–1.28)	0.98 (0.89–1.08)	1.03 (0.83–1.18)
EC$_a$ (mS m^{-1})[b]	6.9 (5.2–9.0)	12.6 (8.8–15.7)	9.4 (5.4–14.3)	15.6 (5.5–58.7)	12.7 (6.0–25.4)	13.2 (6.0–22.0)	13.0 (9.6–16.2)	13.9 (12.0–16.0)	10.3 (9.1–11.6)
RVI[c]	6.9 (5.1–8.5)	9.0 (6.0–11.1)	7.7 (3.8–10.0)	5.8 (4.1–8.1)	7.3 (5.3–9.2)	4.5 (3.4–6.0)	9.2 (7.3–11.3)	10.5 (8.1–13.2)	6.7 (3.4–9.5)
Yara[d]	9.7 (8.7–10.4)	9.6 (8.6–10.4)	8.6 (6.5–9.4)	8.3 (7.6–9.1)	8.8 (7.9–9.5)	7.1 (6.2–8.0)	10.6 (9.6–11.6)	8.6 (7.0–9.9)	–
NDVI[e]	0.74 (0.67–0.79)	0.79 (0.71–0.83)	0.75 (0.57–0.82)	0.69 (0.61–0.78)	0.75 (0.68–0.80)	0.63 (0.54–0.71)	0.80 (0.76–0.84)	0.82 (0.78–0.86)	0.72 (0.54–0.81)

[a]Solar insolation index

[b]Soil apparent electrical conductivity

[c]Ratio vegetation index

[d]Yara N-sensor

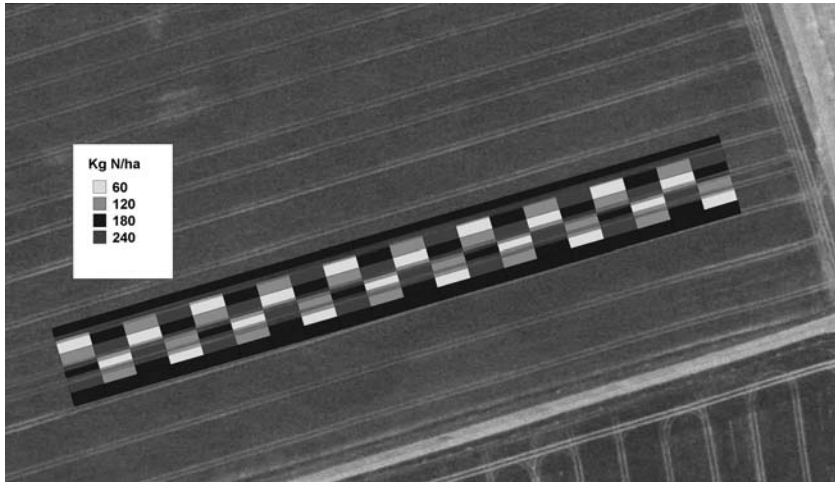[e]Normalized difference vegetation index

Fig. 1 The experimental design for field 1 (Vindum) with layout of gross plots. The experimental design in the other eight fields followed the same general layout. The Vindum trial included 120 plots in 20 rows and 6 columns with a total length of 300 m. The grey scale of each plot represents the N application rate (kg N ha^{-1})

Data recording and processing

The soil and plant observations were obtained using handheld equipment (RVI and other spectral vegetation indices) and vehicle-mounted equipment (EM38, GPS and Yara N biomass). The manual measurements were made with four replicates per plot and averaged to give a representative plot value. For the mobile equipment, two approaches were taken to obtain representative plot values. The soil EC$_a$ and the simultaneous observations of altitude by GPS acquired along transects spaced 12 m apart, were interpolated across the field using an inverse distance weighting method (grid size 4 m, search radius 9 m). The elevation map was used to derive slope and aspect maps. The slope, aspect, and soil EC$_a$ values of grid cells with centers located inside field plots were subsequently averaged. The Yara N biomass observations represented pairs of plots located on both sides of the vehicle. Each pair of plots was assigned the average of biomass values obtained over the length of the plots.

Several topographically derived indices were calculated: a height index based on the absolute height minus the average height of the field, an aspect index defined as the cosine of the aspect angle relative to north, and an index of relative incident solar radiance (solar insolation index, SII) based on fundamental trigonometric relationships (for an overview, see Iqbal, 1983). The SII was defined as:

$$
\begin{aligned}
\text{SII} &= \frac{\cos\theta}{\cos\theta_Z}, \\
\cos\theta &= \cos\varphi\,\cos\beta + \sin\varphi\,\sin\beta\,\cos(\gamma), \\
\cos\theta_Z &= \cos\varphi,
\end{aligned}
\tag{1}
$$

where θ denotes the angle between the surface normal vector and the direction towards the sun, θ_Z denotes the angle between the surface normal vector for flat terrain ($\beta = 0$) and the vector defining the direction towards the sun at solar noon at the equinox, ϕ defines the

latitude in decimal degrees (~56° for Denmark), β and γ denote the surface slope and aspect, respectively, with south defined as $\gamma = 0°$. At mid-latitudes the SII values will range between 0.1 and 1.6 for terrain with slopes between 0 and 30°. Large values represent large relative irradiance values (typically slopes facing south).

Data analysis

The plot grain yield was assumed to be a sum of the following three functions:

1. A function of the N application.
2. A function of the sensor measurement.
3. An interaction between the N application rate and the sensor measurement.

Re point 1. Yield response to N application was described by three different yield functions:

a second order polynomial

$$Y_{ij} = a_i N_{ij}^2 + b_i N_{ij} + c_i, \tag{2}$$

the linear plus exponential (LpE) function

$$Y_{ij} = a_i r_i^{N_{ij}} + b_i N_{ij} + c_i, \tag{3}$$

and the Mischerlich function

$$Y_{ij} = a_i \left(1 - e^{N_{ij}/b_i}\right) + c_i, \tag{4}$$

where Y_{ij} and N_{ij} are the dry matter yield (Mg ha^{-1}) and N application rate (kg N ha^{-1}) in plot j located in field i, respectively. The constants a_i, b_i, c_i and r_i are field specific constants. The statistical analysis was performed using a general nonlinear model (PROC NLIN, SAS 1996).

Re point 2. In fields with a uniform N application rate, the relation between yield and sensor measurements is often linear. However, nonlinear responses have also been observed for example NDVI (Lukina et al., 2001), soil EC$_a$ (Kitchen et al., 2003) and slope (Yang, Peterson, Shropshire, & Otawa, 1998). To facilitate both situations, a second order polynomial was selected to describe the relation between yield and sensor measurement.

Re point 3. After testing the ability of several different functions to describe the effect of the interaction between N application rate and sensor measurements on plot yield, a third order polynomial was selected.

Thus, if a polynomial yield response to N was assumed, the total model describing the yield response to N application and sensor measurement was

$$\begin{aligned} Y_{ij} = {} & a_i N_{ij}^2 + b_i N_{ij} + c_i \\ & + d_i S_{ij} + e_i S_{ij}^2 \\ & + f_i S_{ij} N_{ij} + g_i S_{ij}^2 N_{ij} + h_i S_{ij}^3 N_{ij} \\ = {} & a_i N_{ij}^2 + \left(b_i + f_i S_{ij} + g_i S_{ij}^2 + h_i S_{ij}^3\right) N_{ij} + c_i + d_i S_{ij} + e_i S_{ij}^2, \end{aligned} \tag{5}$$

where S_{ij} is a sensor measurement (e.g. RVI, soil EC_a, Yara Biomass) or a topographic index parameter (i.e. slope, aspect, SII) characterizing plot j located in field i and d_i, e_i, f_i, g_i and h_i are field specific constants.

The total yield from all plots located in field i is thus

$$Y_i^* = \sum_{j=1}^{k_i} Y_{ij}, \tag{6}$$

where k_i is the number of plots located in field i.

Redistribution method

Redistribution of a given amount of N within a single field with the aim of obtaining the greatest yield is equivalent to maximizing Eq. 6 given that

$$\sum_{j=1}^{k_i} N_{ij} = k_i N_i^*, \tag{7}$$

where N_i^* is the average amount of N applied to field i. The appendix describes how N_{ij} is calculated so Eq. 6 is maximized:

$$N_{ij} = N_i^* + \frac{f_i S_{ij} + g_i S_{ij}^2 + h_i S_{ij}^3}{-2a_i} + \gamma_i, \tag{8}$$

where γ_i is a field-specific constant, depending on sensor measurements, adjusted so the field on average receives N_i^* (kg N ha^{-1}). From this equation it follows that a general prediction of N redistribution implies that the constants a_i, f_i, g_i and h_i, should be estimated globally and not as field-specific constants. The other constants can be estimated for each field.

Economically optimal method

Another method for variable N application is to estimate the economically optimal N application for each plot. Algorithms for this purpose can also be estimated from Eq. 5 by noting that the economically optimal N application must satisfy the following equation:

$$\frac{\partial Y_{ij}}{\partial N_{ij}} = \lambda, \tag{9}$$

where λ is the ratio of grain and N fertilizer prices. This ratio is quite variable and depends on the actual market price. In this study, we have chosen a value of 0.2 (Pedersen, 2002). By differentiating Eq. 5 the optimal N_{ij} value can be calculated as

$$N_{ij} = \frac{\lambda - \left(b_i + f_i S_{ij} + g_i S_{ij}^2 + h_i S_{ij}^3\right)}{2a_i}. \tag{10}$$

To make this algorithm generally applicable, the constants a_i, b_i, f_i, g_i and h_i need to be estimated as global parameters. Thus, compared with the redistribution method an extra parameter (b_i) needs to be estimated for all fields.

Combinations of measurements from several sensors were analyzed using the approach outlined above by including two sensor terms and a single interaction term between the two sensors and the N application rate:

$$
\begin{aligned}
Y_{ij} \ &= a_i N_{ij}^2 + b_i N_{ij} + c_i + d_i S_{ij} + e_i S_{ij}^2 + f_i S_{ij} N_{ij} + g_i S_{ij}^2 N_{ij} \\
&+ h_i T_{ij} + i_i T_{ij}^2 + j_i T_{ij} N_{ij} + l_i T_{ij}^2 N_{ij} + m_i S_{ij} T_{ij} N_{ij},
\end{aligned}
\tag{11}
$$

where S_{ij} and T_{ij} are different sensor measurements in plot j located in field i. All statistical analyses were performed using a general linear model (PROC GLM, SAS, 1996).

Methods for maximizing N uptake and minimizing variation in protein content

Crop N uptake and protein content for each plot were also estimated using Eq. 5 as outlined above, by substituting Y_{ij} with the measured N uptake or protein content in plot j located in field i. Algorithms for the redistribution of N to obtain the largest crop N uptake is then calculated from Eq. 8. For protein content, where the aim is to minimize variation, a different approach was taken. The aim is to minimize

$$
\sum_{j=1}^{k_i} (P_{ij} - P_i^*)^2,
\tag{12}
$$

where P_{ij} is the estimated protein content in plot j located in field i and P_i^* is the estimated average protein content for field i. This equation cannot be minimized analytically, so the optimal N application rate that minimizes Eq. 12 given Eq. 7 was estimated numerically using Microsoft Excel Solver. It is noted that to minimize Eq. 12, it is necessary to estimate a_i, b_i, d_i, e_i, f_i, g_i and h_i as global rather than field-specific parameters.

Results

Data

The mean and variation in yield, protein content, N uptake, topographic indices and sensor measurements for each field are given in Table 2. The large observed variation in yield, protein content and N uptake could be attributed primarily to the four levels of N fertilizer application. Variation in topographic indices was observed in fields four and seven. The soil EC_a measurements indicated that fields four, five and six were the most variable with respect to soil texture. Based on plant sensor measurements, no single field appeared to be significantly more variable than the rest.

Interactions between N application rate and crop yield

In general, the second order polynomial (Eq. 2) described the yield response to N better than the LpE or the Mischerlich model (Eqs. 3, 4, data not shown). For fields four and nine only was the variation explained better by Eq. 4 or 3, respectively. Therefore, we decided to use the second order polynomial model in the remaining part of the analysis. The parameters estimated for the second order polynomial model (Eq. 2) are given in Table 3 for the individual fields. There was a significant correlation between yield and N application for all fields, except for field nine; this was excluded from further analysis. The large weed population within this field was also likely to affect the relations between yield and

Table 3 Parameter estimates, r^2 and root mean square error (RMSE) for yield response to N application (Eq. 2) for the individual fields

Field	$a \times 10^{-3}$	b_i	c_i	r^2	RMSE (Mg ha^{-1})
1	−0.85	0.38	60	0.78	0.38
2	−0.90	0.35	57	0.51	0.52
3	−0.95	0.45	39	0.64	0.92
4	−0.47	0.22	26	0.57	0.39
5	−1.20	0.46	26	0.41	0.84
6	−0.64	0.37	16	0.42	1.14
7	−0.72	0.25	56	0.16	0.66
8	−0.44	0.16	60	0.13	0.51
9	ns	ns	67	0.01	1.25

ns = not significant at a 5% level

canopy sensor measurements. The root mean squared error of the yield response for the individual fields varied between 0.39 and 1.25 Mg ha^{-1}.

Figure 2 shows the yield response to N application rates for field six. The yield is subdivided into classes according to the RVI measurements made before the application of N. The figure shows that the yield is related to both N application rate and plant sensor measurements. In addition, the estimated yield response based on Eq. 5 is shown for three selected RVI levels.

Interactions between sensor measurements and crop yield

The effect of including plant or soil sensors, or topographic information to predict crop yield is given in Table 4. The first two lines in Table 4 give the statistics of the total model
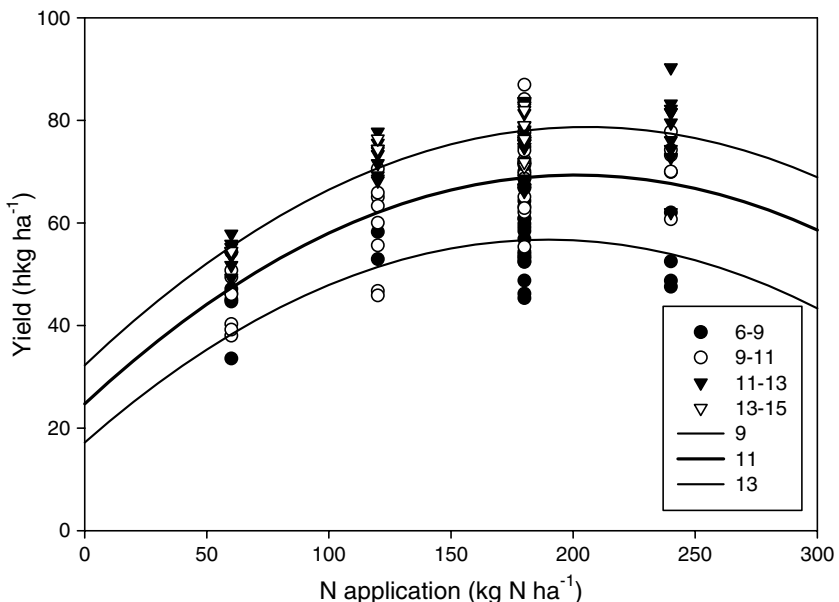

Fig. 2 Grain yield plotted against N application rate for field 6. The symbols represent RVI intervals measured before N application. Modeled yield response based on Eq. 5 are shown for three selected levels of RVI

Table 4 Parameter estimates, r^2 and root mean square error (RMSE) for Eq. 5 based on different sensor measurements

Sensor	$a \times 10^{-3}$	f	g	h	r^2	RMSE (Mg ha^{-1})
Site N	–	–	–	–	0.79	0.745
Global N	−0.82	–	–	–	0.79	0.746
RVI	−0.81	0.098	-0.011	0.00036	0.90	0.500
Yara	−0.85	0.41	-0.041	0.00131	0.89	0.543
NDVI	−0.81	3.07	-2.04	ns	0.91	0.497
EC$_a$	−0.83	0.0046	-2.77×10^{-4}	3.4×10^{-6}	0.84	0.648
Height[1]	−0.83	0.0025	ns	ns	0.81	0.710
Slope[1]	−0.75	ns	ns	ns	0.83	0.653
SII[1]	−0.76	ns	ns	ns	0.83	0.655
Aspect	−0.76	ns	ns	ns	0.83	0.657

The first two rows show the site specific and global N response, both based on Eq. 2

[1]Without data from field 3. ns = not significant at a 5% level

(Eq. 5) where a_i is estimated either for each field or for the whole data set. All canopy and soil sensor measurements improved the prediction of crop yield.

The topographic information improved the description of yield variation only slightly compared with the basic yield function. For most of the topographic indices (slope, SII and aspect) the f, g and h parameters were not significant at the 5% level. Thus, there was no significant interaction between the N rate and these topographic indices and it was not possible to develop algorithms based on Eq. 8 using these indices. However, for the height index there was a significant interaction between sensor measurement, N application and crop yield, as f was significant at the 5% level.

Several combinations of plant and soil sensor measurements, or topographic information were tested (data not shown). However, only combinations that included soil EC$_a$ improved the predictions. Table 5 gives the parameters and statistics of a model that combines either the RVI or the Yara N-sensors and soil EC$_a$ based on Eq. 11.

Parameters for the relation between N uptake and protein content, and selected sensor measurements are given in Table 6. The other sensors and topographic indices did not describe the protein content and N data as well as RVI, Yara and EC$_a$ (data not shown).

Algorithms for N redistribution

Several algorithms for optimizing yield by redistribution of N based on different sensors were developed (Fig. 3). These algorithms were based on Eq. 8 and parameter estimates from Table 4. As an example, the RVI algorithm was based on the f, g and h parameters (Table 4) and inserted in Eq. (8). To estimate γ_i in this equation we assumed a uniform frequency distribution of the sensor measurements (between 5 and 11) on the x-axis. Therefore, in fields with different distributions of sensor measurements, the algorithms will have the same form but with a different N level (i.e. different γ_i values). Algorithms for the other sensors were developed using the same approach. In addition, algorithms for optimizing N uptake and minimizing the protein content (Fig. 3) were developed based on Table 6. For algorithms based on sensor combinations (Fig. 4), the parameter estimates were taken from Table 5.

In general, the algorithms moved N from areas with large and small sensor values to areas with intermediate values. The algorithms developed reflect their objective: to maximize yield and N uptake, or to minimize variation in protein content. In general, the

Table 5 Parameter estimates, r^2 and root mean square error (RMSE) for a model based on the combination of selected sensors (Eq. 11)

Sensor	$a \times 10^{-3}$	f	g	j	l	m	r^2	RMSE (Mg ha^{-1})
RVI* EC$_a$	−0.83	0.039	-0.0016	0.0052	ns	−0.00072	0.91	0.487
Yara* EC$_a$	−0.86	0.093	-0.0043	0.018	-4.5×10^{-5}	−0.0018	0.90	0.527

Table 6 Parameter estimates, r^2 and root mean square error (RMSE) for N uptake and protein content based on Eq. 5

Sensor	$a \times 10^{-3}$	f	g	h	r^2	RMSE
N uptake						
Site N	–	–	–	–	0.85	14.1
Global N	−0.0013	–	–	–	0.85	14.2
RVI	−0.0012	0.18	−0.018	0.00061	0.92	10.2
Yara	−0.0013	0.84	−0.084	0.0027	0.92	10.7
EC$_a$	−0.0013	0.018	−8.1×10^{-4}	8.9·10^{-6}	0.88	12.8
Protein content						
Site N	–	–	–	–	0.85	0.64
Global N	−3.4×10^{-5}	–	–	–	0.83	0.68
RVI	−2.3×10^{-5}	−6.9×10^{-3}	7.6×10^{-4}	−2.5·10^{-5}	0.83	0.70
Yara	−2.7×10^{-5}	−6.9×10^{-3}	3.1×10^{-4}	−1.2·10^{-6}	0.83	0.70
EC$_a$	−3.3×10^{-5}	−6.0×10^{-4}	2.7×10^{-5}	−2.6·10^{-7}	0.83	0.68

RMSE in kg N ha^{-1} and % for N uptake and protein content, respectively

optimal value for the yield algorithms is smaller than that for the N uptake algorithm, which in turn is smaller than the optimal value of the protein content algorithm (Fig. 3).

For the combination of the EC$_a$ and the Yara N-sensors (Fig. 4), the results show an interaction between the Yara N-sensor value and the soil EC$_a$ value. Thus, for the more clayey parts of the field (large EC$_a$ values) the model predicted that the crops that should receive the largest N application had a Yara N-sensor value of about seven, whereas in the more sandy parts of the field (small EC$_a$ values) the optimal Yara N value was close to 10.

Redistribution vs. economic optimum algorithms

As noted in the materials and methods section, the economically optimal algorithm requires the estimation of an extra global parameter (b_i) in Eq. 5 compared with the redistribution algorithms. Based on Eq. 10 the average economically optimal N rate for each field (Table 7) can be calculated based on either the local N response (parameters from Eq. 2), the redistribution method (parameters from Eq. 5) or the economically optimal method (parameters from Eq. 5). The local N response was similar to the redistribution method with large differences between fields. In contrast, the economically optimum method predicted quite different optimal values with less variation between fields.

Yield increase

The theoretical yield increase resulting from the redistribution methods can be calculated using the sensor measurements obtained from the nine fields. It was assumed that 180 kg N ha^{-1} should be redistributed within each field. First, the N application rates were calculated using Eq. 8 and sensor measurements. The yield was then estimated from Eq. 5
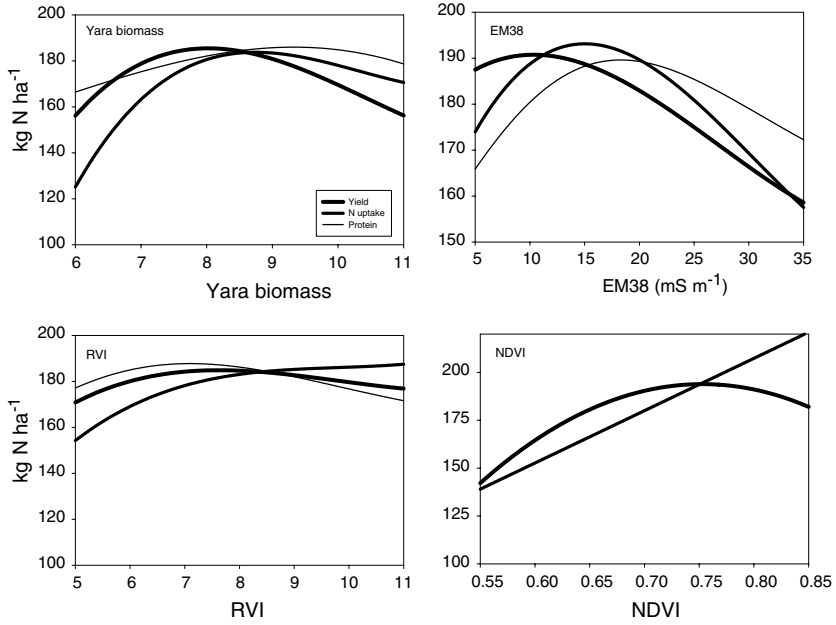
Fig. 3 Optimal redistribution of N based on sensor measurements of Yara, EC_a, RVI or NDVI. Lines represent the yield, N and protein content algorithms, respectively. Note different scales for both axes
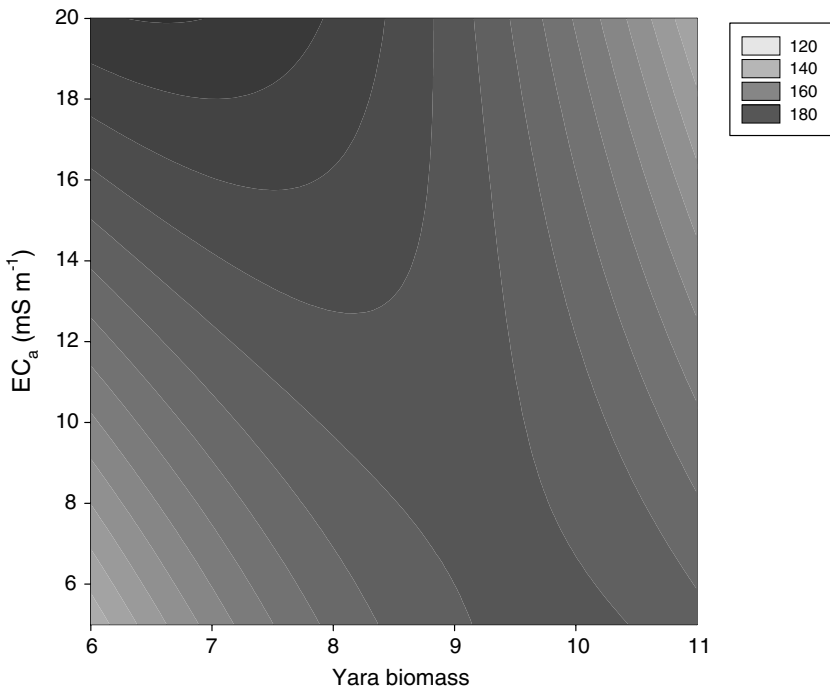

Fig. 4 Optimal redistribution of N fertilizer (kg N ha^{-1}) based on a combination of RVI and EC_a

Table 7 Economically optimal N application (kg N ha^{-1}) based on different application models

Field	N model	Redistribution	Economic optimum
1	104	102	87
2	84	78	65
3	134	132	77
4	17	72	92
5	111	96	83
6	128	137	93
7	33	47	64
8	0	40	51

See text for description of the models

and the N application rate was calculated. To estimate a yield increase, the yield obtained from applying 180 kg N ha^{-1} uniformly was calculated based on the same equations and sensor measurements as above. The average increase in yield, N uptake, or reduction in protein content variation in all the fields based on different sensors is given in Table 8. It shows that the estimated theoretical increase in yield, N uptake and reduction in the variation of protein content are small.

Discussion

For the Yara algorithm, N fertilizer was moved from areas with small and large sensor values to those with intermediate values. An explanation for this might be that areas with low Yara biomass represent areas with low tiller density or some other crop abnormality that reduces the yield response to N. In areas with high Yara biomass, the conditions are more favorable for a high rate of productivity without extra N application. This might be due to a high rate of soil N mineralization, which will reduce the yield response to N application. For the yield algorithm, an optimal Yara value close to eight was estimated. However, the optimal Yara value depends on whether the aim is to maximize yield, N uptake or to reduce variation in protein concentration (Fig. 4). For the N uptake algorithm, the optimal Yara value is larger than for the yield algorithm. This is because areas with a large Yara value represent areas with high biomass and a greater capacity for N uptake than other areas. Thus, if the aim is to optimize the N uptake it is advantageous to increase N application in relation to higher Yara biomass values than for the yield algorithm. For the protein content algorithm, the redistribution of N also benefits the higher biomass areas, which tend to have large yields but low protein contents. The response curves for the other plant sensors were similar to that of the Yara sensor. Small EC$_a$ values indicate sandy areas

Table 8 Estimated average theoretical increase in grain yield and N uptake or reduction in the variation in protein content based on algorithms for selected sensor measurements from all experimental fields

	Yield increase (Mg ha^{-1})	N uptake increase (kg N ha^{-1})	Reduced variation in protein content (%)
RVI	0.004	0.16	0.17
Yara	0.004	0.08	0.16
EC$_a$	0.008	0.17	0.21

with low productivity, whereas large values tend to be more productive because of the larger clay content.

Other authors and companies have developed methods for variable-rate N application. The commercial Yara N-sensor system used in this study estimates a biomass level and provides a recommendation for the redistribution of N fertilizer. Figure 5 shows the N recommendation from the Yara N-tester plotted against the N application predicted from Eq. 8, based on Yara biomass estimates. In eight out of nine fields, the estimated N application rates are similar for the two methods. The algorithm for converting Yara biomass to N application embedded in the commercial system is not available, making it difficult to explain why the two algorithms respond differently for field six. This field has particularly low Yara biomass values (Table 2), therefore, it is hypothesized that the difference between the methods depends on how very small biomass values are handled.

Flowers et al. (2003) and Welsh et al. (1999) developed algorithms for predicting N demand based on NDVI measurements. Both studies predict smaller N applications with increasing NDVI values. This was also observed in the current study for large NDVI values (Fig. 3). However, the previous authors did not have small NDVI values that would require low N application rates. Hansen, Skjødt, and Jørgensen (2003) also developed an algorithm based on NDVI. For the second application of N fertilizer, they estimated that the rates would decrease for both large and small NDVI values.

Several authors (e.g. Jiang & Thelen, 2004; Yang et al. 1998; Vrindts et al. 2003) have observed significant relations between yield and topography within a field. However, those observed in our study were both positive and negative (data not shown) and there was no general significant interaction between N application and most topographic indices. Algorithms based on topography were only possible for the height index (Table 4). From Table 4 and Eq. 8 it was estimated that the N application rate should be increased by 1.5 kg N ha^{-1} for every 1 m increase in height. From an agronomical point of view, this
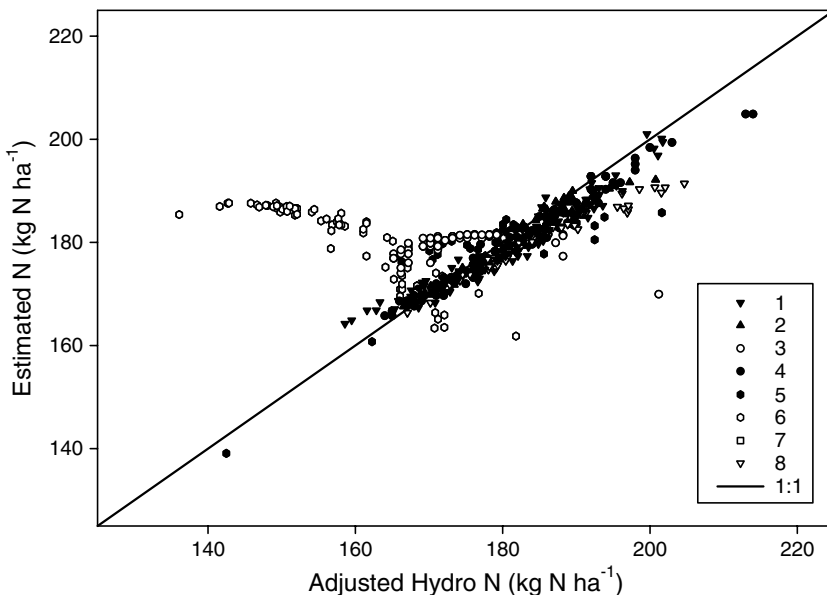

Fig. 5 Yara N recommended N application rate and optimal N application estimated from Eq. 8. The Yara N recommendations have been adjusted so total N application rate equals the method based on Eq. 8. Symbols represent the eight field sites

increase is plausible, as erosion tends to move organic matter from higher to lower elevations. Therefore, N mineralization is generally greater at lower elevations compared with higher ones.

Different approaches can be used to estimate the incoming radiation based on topography. The current study uses an index of potential incoming solar radiation. Based on this index, no general conclusion on the influence of radiation on yield variation could be made since only one field had a positive correlation between SII and yield, whereas two had a negative one (data not shown). In a simulation study by Reuter, Wendroth, Kersebaum, and Schwarz (2001), which estimates the actual daily radiation, yield predictions were improved by including radiation.

The estimated increase in yield in this study was close to zero. Thus, the increase in grain yield obtained by moving a kilo of N from less fertile to more fertile areas was too small to obtain an overall increase in grain yield. This small or zero increase in yield has also been observed in tests with the Yara N-sensor (e.g. Pedersen, 2002). In addition, several other tests of algorithms showed no increase in yield (e.g., Ebertseder, Gutser, Hege, Brandhuber, & Schmidhalter 2003; Flowers et al., 2003; Hansen et al., 2003; Vrindts et al., 2003). In a review of 17 studies of variable N, P and K application rates by Lowenberg and Swinton (1997) five were unprofitable, six were intermediate and six were profitable.

A possible explanation for the small predicted increase in yield is that the experimental design was not optimal for determining the relations between yield and sensor measurements. Several growth factors interact to determine the final yield of a winter wheat crop. In years with no water stress, a south-facing slope is advantageous, whereas it may be a disadvantage in years with water stress. Several well-known and less well-known relations exist that determine the final yield. These relations might blur the estimated effects and thereby give rise to a small predicted increase in yield. With an empirical approach such as ours it is not possible to include such relations, unless the data set were much larger and covered a wider range of climatic and soil conditions. An alternative approach would be to use dynamic simulation models to describe the relations. However, such models require a large number of input data including a good description of soil properties. In addition, models that can handle both topographic information as well as detailed information on soil and crop properties are not well tested.

Adjacent plots or those close to each other that received the same rate of N could have very different levels of yield (data not shown). This was not explained by differences in sensor measurements; therefore, there might be a problem with the size of plot. Solie, Raun, and Stone (1999) estimated that plots less than 1 m^2 are necessary for the quantification of the most optimal N application rate. However, this small resolution cannot be achieved in current commercial farming systems and was impossible to implement practically in the current experiment. In addition, the study by LaRuffa et al. (2001) did not show any significant correlations between plot size (from 0.84 to 53.51 m^2), yield and N rate over a 3-year period.

The difference between developing a redistribution algorithm and an economic optimum one is illustrated clearly in Table 7. Estimation of the extra parameter in the economic optimum algorithm implies that inter-field variation is predicted less well than for the redistribution methods. In particular, the estimated range in N application (51–93 kg N ha^{-1}) is less than the range estimated by a local N response (0–134 kg N ha^{-1}). Thus, the redistribution algorithms will theoretically give better results, but they require that the average N application is determined by other means. Traditionally this is achieved by balance sheet methods or by estimating the residual N effects of preceding crops, pastures, organic manures, etc.

Conclusions

Several methods for the redistribution of N fertilizer based on different sensor measurements were developed to: maximize yield, maximize N uptake and minimize the variation in protein content. In general, the algorithms moved N from areas with relatively small or large sensor values to intermediate areas with an ''optimal'' sensor value. Considering all algorithms, the optimal yield algorithm resulted in the smallest optimal sensor value, and the algorithm for uniform protein content resulted in the largest one.

The theoretical benefits resulting from using the algorithms described were too small, however, to warrant their implementation in practice. The limited benefits are due to the limited capability of the currently available sensors to predict yield at harvest.

Based on the above, it seems that more focus should be directed towards describing inter-field variation rather than intra-field variation. Inter-field variation might be described using precision technologies such as satellite or aerial imagery. In addition, improved or new sensors that describe additional crop (e.g. LAI and canopy structure) or soil features (e.g. organic matter, relative water content) might provide a better relationship between sensor measurements and the achieved grain yield.

Appendix A

This appendix describes how to maximize yield (Eqs. 5, 6) given a fixed N application rate (Eq. 7). From Eq. 7 it can be seen that the N_{ij}'s depend on each other. Thus, simultaneous maximization of Eqs. 6, 7 is not immediately possible. However, Eq. (6) can be rearranged to

$$N_{ik_i} = k_i N_i^* - \sum_{j=1}^{k_i-1} N_{ij}. \tag{13}$$

Eqs. 5, 6 can now be reduced to

$$
\begin{aligned}
Y_i^* &= \sum_{j=1}^{k_i-1} Y_{ij} + Y_{ik_i} \\
&= \sum_{j=1}^{k_i-1} \left(a_i N_{ij}^2 + \left(b_i + f_i S_{ij} + g_i S_{ij}^2 + h_i S_{ij}^3 \right) N_{ij} + c_i + d_i S_{ij} + e_i S_{ij}^2 \right) \\
&\quad + \left(a_i \left(k_i N_i^* - \sum_{j=1}^{k_i-1} N_{ij} \right)^2 + \left(b_i + f_i S_{ik_i} + g_i S_{ik_i}^2 + h_i S_{ik_i}^3 \right) \left(k_i N_i^* - \sum_{j=1}^{k_i-1} N_{ij} \right) + c_i + d_i S_{ik_i} + e_i S_{ik_i}^2 \right).
\end{aligned}
\tag{14}
$$

This equation is simplified by setting $\alpha_{ij} = \left(b_i + f_i S_{ij} + g_i S_{ij}^2 + h_i S_{ij}^3 \right)$:

$$Y_i^* = \sum_{j=1}^{k_i-1} \left(a_i N_{ij}^2 + \alpha_{ij} N_{ij} + c_i + d_i S_{ij} + e_i S_{ij}^2 \right) +$$
$$+ \left(a_i \left(k_i N_i^* - \sum_{j=1}^{k_i-1} N_{ij} \right)^2 + \alpha_{ik_i} \left(k_i N_i^* - \sum_{j=1}^{k_i-1} N_{ij} \right) + c_i + d_i S_{ik_i} + e_i S_{ik_i}^2 \right). \tag{15}$$

In this equation the N_{ij}'s are independent and Y_i^* can be maximized by setting the partial derivative of Y_i^* with respect to N_{ij} to zero:

$$\frac{\partial Y_i^*}{\partial N_{ij}} = 0. \tag{16}$$

Eq. (15) is now differentiated and inserted into Eq. (16):

$$2a_i N_{ij} + \alpha_{ij} - 2a_i \left(k_i N_i^* - \sum_{j=1}^{k_i-1} N_{ij} \right) - \alpha_{ik_i} = 0. \tag{17}$$

This equation is solved with respect to N_{ij} using Eq. (13).

$$N_{ij} = \frac{-1}{2a_i} \left(\alpha_{ij} - 2a_i N_{ik_i} - \alpha_{ik_i} \right). \tag{18}$$

Combining this equation with Eq. (13) gives

$$N_{ik_i} = k_i N_i^* - \sum_{j=1}^{k_i-1} N_{ij} = k_i N_i^* - \sum_{j=1}^{k_i-1} \frac{-1}{2a_i} \left(\alpha_{ij} - 2a_i N_{ik_i} - \alpha_{ik_i} \right)$$
$$= k_i N_i^* - (k_i - 1) N_{ik_i} + \sum_{j=1}^{k_i-1} \left(\frac{\alpha_{ij} - \alpha_{ik_i}}{2a_i} \right). \tag{19}$$

This equation is then solved with respect to N_{ik_i}

$$N_{ik_i} = \frac{1}{k_i} \left(k_i N_i^* + \sum_{j=1}^{k_i-1} \left(\frac{\alpha_{ij} - \alpha_{ik_i}}{2a_i} \right) \right) = N_i^* + \sum_{j=1}^{k_i-1} \left(\frac{\alpha_{ij} - \alpha_{ik_i}}{2a_i k_i} \right). \tag{20}$$

Finally, this is inserted into Eq. (18)

$$N_{ij} = N_i^* + \sum_{j=1}^{k_i-1} \left(\frac{\alpha_{ij} - \alpha_{ik_i}}{2a_i k_i} \right) - \frac{\alpha_{ij} - \alpha_{ik_i}}{2a_i}$$
$$= N_i^* + \frac{1}{2a_i} \left(\sum_{j=1}^{k_i-1} \left(\frac{\alpha_{ij} - \alpha_{ik_i}}{k_i} \right) - \alpha_{ij} + \alpha_{ik_i} \right) \tag{21}$$
$$= N_i^* + \frac{1}{2a_i} \left(-\alpha_{ij} + \sum_{j=1}^{k_i} \frac{\alpha_{ij}}{k_i} \right).$$

Expanding α_{ij} gives

$$N_{ij} = N_i^* + \frac{1}{2a_i}\left(-\left(b_i + f_iS_{ij} + g_iS_{ij}^2 + h_iS_{ij}^3\right) + \sum_{j=1}^{k_i}\frac{\left(b_i + f_iS_{ij} + g_iS_{ij}^2 + h_iS_{ij}^3\right)}{k_i}\right). \quad (22)$$

To obtain a global model of how to redistribute N based on a sensor measurement (S_{ij}), it is evident from the above equation that a_i, f_i, g_i and h_i cannot be estimated for each field but must be determined as common factors for all experiments. It is also noted that b_i and the sum are constants within a single field, which implies that Eq. (22) can be rewritten as

$$N_{ij} = N_i^* + \frac{f_iS_{ij} + g_iS_{ij}^2 + h_iS_{ij}^3}{-2a_i} + \gamma_i. \quad (23)$$

Under field conditions γ_i can be determined by noting that

$$\begin{aligned}\sum_{J=1}^{k_i} N_{ij} &= \sum_{J=1}^{k_i}\left(N_i^* + \frac{f_iS_{ij} + g_iS_{ij}^2 + h_iS_{ij}^3}{-2a_i} + \gamma_i\right) \\ &= k_iN_i^* + k_i\gamma_i + \sum_{J=1}^{k_i}\left(\frac{f_iS_{ij} + g_iS_{ij}^2 + h_iS_{ij}^3}{-2a_i}\right),\end{aligned} \quad (24)$$

and by combining Eqs. 6, 22 the following expression is obtained:

$$\gamma_i = \frac{-1}{k_i}\sum_{j=1}^{k_i}\left(\frac{f_iS_{ij} + g_iS_{ij}^2 + h_iS_{ij}^3}{-2a_i}\right). \quad (25)$$

References

Baden, G., Williams, A., & Hoey, D. (1987). The use of electromagnetic induction to detect the spatial variability of salt and clay content of soils. *Australian Journal of Soil Resources, 25,* 21–27.

Ebertseder, Th., Gutser, R., Hege, U., Brandhuber, R., & Schmidhalter, U. (2003). Strategies for site specific nitrogen fertilisation with respect to long-term environmental demands. In J. Stafford, & A. Werner (Eds.), *Precision agriculture* (pp. 193–198). Wageningen: Academic Publishers.

Flowers, M., Weisz, R., & Heiniger, R. (2003). Quantitative approaches for using color infrared photography for assessing in-season nitrogen status in winter wheat. *Agronomy Journal, 95,* 1189–1200.

Greve, M. H., Nehmdahl, H., & Krogh, L. (2003). Soil mapping on the basis of soil electric conductivity measurements with EM38. In B. Linden, & S. E. Olesen (Eds.), *Implementation of precision farming in practical agriculture* (pp. 26–34). Denmark: Dias report no 100, Danish Institute of Agricultural Science.

Hansen, P. M., Skjødt, P., & Jørgensen, R. N. (2003). Algorithm for variable nitrogen rate—application in winter wheat. In B. Linden, & S. E. Olesen (Eds.), *Implementation of precision farming in practical agriculture* (pp. 56–64). Denmark: Dias report no 100, Danish Institute of Agricultural Science.

Heiniger, R. W., McBride, R. G., & Clay, D. E. (2003). Using soil electrical conductivity to improve nutrient management. *Agronomy Journal, 95,* 508–519.

Iqbal, M. (1983). *An introduction to solar irradiation.* USA: Academic Press Inc.

Jiang, P., & Thelen, K. D. (2004). Effects of soil and topographic properties on crop yield in a north-central corn–soybean cropping system. *Agronomy Journal, 96,* 252–258.

Joernsgaard, B., & Halmoe, S. (2003). Intra-field yield variation over crops and years. *European Journal of Agronomy, 19,* 23–33.

Kitchen, N. R., Drummond, S. T., Lund, E. D., Sudduth, K. A., & Buchleiter, G. W. (2003). Soil electrical conductivity and topography related to yield for three contrasting soil–crop systems. *Agronomy Journal, 95*, 483–495.

LaRuffa, J. M., Raun, W. R., Phillips, S. B., Solie, J. B., Stone, M. L., & Johnson, G. V. (2001). Optimum field element size for maximum yields in winter wheat, using variable nitrogen rates. *Journal of Plant Nutrition, 24*, 313–325.

Lowenberg-DeBoer, J., & Swinton, S. (1997). Economics of site-specific management in agronomic crops. In P. Robert, R. Rust, & W. Larson (Eds.), *The state of site-specific management for agriculture: Proceedings of the 3rd international conference on precision agriculture*, Madison, WI, USA, pp. 369–396.

Lund, E. D., Wolcott, M. C., & Hanson, G. P. (2001). Applying nitrogen site-specifically using soil electrical conductivity maps and precision agriculture technology. *The Scientific World, 1*, 767–776.

Lukina, E. V., Freeman, K. W., Wynn, K. J., Thomason, W. E., Mullen, R. W., Stone, M. L., Solie, J. B., Klatt, A. R., Johnson, G. V., Elliott, R. L., & Raun, W. R. (2001). Nitrogen fertilization optimization algorithm based on in-season estimates of yield and plant nitrogen uptake. *Journal of Plant Nutrition, 24*, 885–898.

Pedersen, C. A. (2002). *Oversigt over Landsforsøgene (in Danish)*. Denmark: Danish Agricultural Advisory Service.

Raun, W. R., Solie, J. B., Johnson, G. V., Stone, M. L., Mullen, R. W., Freeman, K. W., Thomason, W. E., & Lukina, E. V. (2002). Improving nitrogen use efficiency in cereal grain production with optical sensing and variable rate application. *Agronomy Journal, 94*, 815–820.

Reuter, H. I., Wendroth, O., Kersebaum, K. C., & Schwarz, J. (2001). Solar radiation modelling for precisions farming—a feasible approach for better understanding variability of crop production. In G. Grenier, & S. Blackmore (Eds.), *Third European conference on precision agriculture* (pp. 845–850). Montpellier, France: ECPA.

SAS Institute (1996). *SAS/STAT software: Changes and enhancements through release 6.11*. Cary, NC, USA: SAS Institute Inc.

Solie, J. B., Raun, W. R., & Stone, M. L. (1999) Submeter spatial variability of selected soil and Bermudagrass production variables. *Soil Science Society of America Journal, 63*, 1724–1733.

Vrindts, E., Reyniers, M., Darius, P., De baerdemaeker, J., Gilot, M., Sadaoui, Y., Frankinet, M., Hanquet, B., & Destain, M.-F. (2003). Analysis of soil and crop properties for precision agriculture for winter wheat. *Biosystems Engineering, 85*, 141–152.

Wollring, J., Reusch, S., & Karlsson, C. (1998). *Variable nitrogen application base on crop sensing. Proceedings No. 423*. UK: The International Fertiliser Society.

Welsh, J. P., Wood, G. A., Godwin, R. J., Taylor, J. C., Earl, R., Blackmore, B. S., Spoor, G., & Thomas, G. (1999). Developing strategies for spatially variable nitrogen application. In J. V. Stafford (Ed.), *Precision agriculture '99: Proceedings of the 2nd European conference on precision agriculture*. Sheffield, UK: Sheffield Academic Press.

Yang, C., Peterson, C. L., Shropshire, G. J., & Otawa, T. (1998). Spatial variability of field topography and wheat yield in the Palouse region of the Pacific Northwest. *Transactions of the ASAE, 41*, 17–27.

Zadoks, J. C., Chang, T. T., & Konzak, C. F. (1974). A decimal code for the growth stages of cereals. *Weed Research, 14*, 415–421.